

Stark widths, shifts, and regularities for Kr II visible spectral lines

J. A. del Val

Departamento de Física Aplicada, EU Politécnica, Universidad de Salamanca, 05071 Ávila, Spain

R. J. Peláez, S. Mar, F. Rodríguez, V. R. González, A. B. Gonzalo, A. del Castro, and J. A. Aparicio
Departamento de Física Teórica, Atómica y Óptica, Universidad de Valladolid, 47071 Valladolid, Spain

(Received 30 October 2007; published 4 January 2008)

Stark widths and shifts of 35 singly charged krypton ion spectral lines have been measured in a pulsed discharge lamp, where electron density ranges from $0.35\text{--}0.8 \times 10^{23} \text{ m}^{-3}$ and electron temperature ranges from 15000–27000 K. This work extends a previous one [A. de Castro *et al.*, *J. Phys. B: At. Mol. Opt. Phys.* **34**, 3275 (2001)] already published by our laboratory. Intramultiplet and intratransition nonregularities have been found and have been explained by considering the perturbing levels effect on the Stark parameters for each one of the measured spectral lines.

DOI: 10.1103/PhysRevA.77.012501

PACS number(s): 32.70.Jz, 32.30.Jc, 32.60.+i

I. INTRODUCTION

Krypton is present in many light sources and lasers as the working gas. Moreover, krypton has been detected in the spectra of the interstellar medium [2], galactic disk [3] and planetary nebulae [4]. In this last case, the spectral information is used to understand the latest stages of the stellar evolution and nucleosynthesis processes [4]. When the Stark broadening is the principal pressure broadening mechanism in plasmas (as is the case of the electron density range of this experiment), it is possible to obtain from observed Stark width and shift values the main plasma parameters as electron temperature and density, essential for the stellar atmospheres modelling. Thus, the knowledge of the Stark broadening parameters (the width and the shift) of ionized krypton spectral lines as functions of electron density and temperature is of great interest for plasma diagnostic purposes.

In the case of Stark parameters in Kr II, there is still a great lack of data, especially in temperature intervals above 17000 K [5]. This makes difficult comparisons and validation of theoretical models. In a previous work already published [1] our laboratory gives Stark widths and shifts of 25 Kr II lines. In that previous work we provided three data for Stark widths and 21 data relative to Stark shift. In the present work, we give Stark widths and shift of 35 Kr II lines selected from an emission experiment [6], and we provide 27 data for Stark widths and 17 data for Stark shifts.

The present results are obtained from measurements performed in a pulsed discharge lamp, with a pure flow of Krypton at a pressure for which self-absorption effects are minimized. Profiles of Kr II spectral lines have been registered at several instants within the plasma life, that is, in different conditions of electron density and temperature. The electron densities have been measured with two-wavelength interferometry, and the temperatures have been obtained from Boltzmann plots of some Kr II lines. The influences of other broadening mechanisms have also been taken into account, such as Doppler broadening and the instrumental function.

For every spectral line, Stark widths and shifts have been plotted as a function of electron density and their values at 10^{23} m^{-3} have been tabulated and compared with the scarce data available in the literature. Only for eight spectral lines

can we compare our measurements with data of other authors, such as the theoretical values of Popovic *et al.* [7] calculated by using a modified semiempirical approach, the experimental values of Milosavljevic *et al.* [8], and the measurements of Bertucelli *et al.* [9]. Reasonable agreement exists between results from Popovic *et al.* [7] and Milosavljevic *et al.* [8], and between some values of Popovic *et al.* [7] and the values of this work. However, some important discrepancies appear between experimental results from Milosavljevic *et al.* [8] and Bertucelli *et al.* [9], and also between these references and our measured values. Important intramultiplet and intratransition nonregularities of the Stark parameters have been detected and explained by taking into account the perturbing levels effects.

II. EXPERIMENTAL ARRANGEMENT

All measurements have been made in a pulsed discharge lamp. The experimental arrangement is shown in Fig. 1.

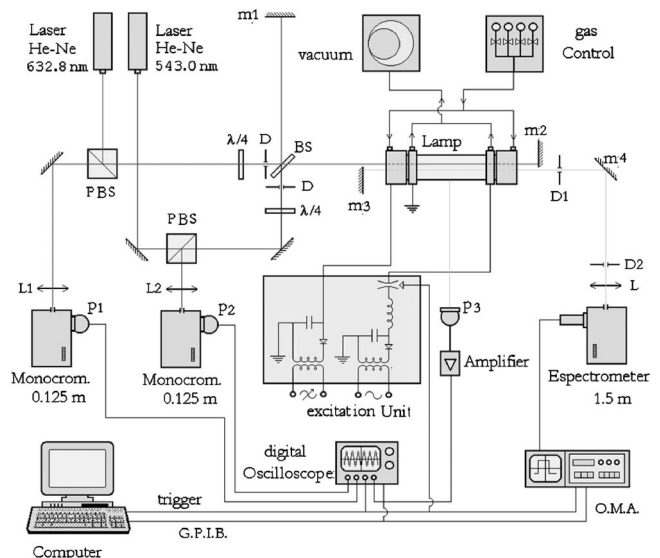


FIG. 1. Experimental arrangement.

More details about the plasma source and plasma diagnostics are given in previous works [10,11]. Thus, we only summarize here the most relevant details concerning this experiment.

The plasma source consists of a cylindrical tube of Pyrex glass, 175 mm in length and 19 mm in interior diameter. The lamp has been designed to avoid sputtering as much as possible. The plasmas were created by discharging a capacitor bank of 20 μF charged up to 7.5 kV. During the whole experiment the lamp was working with a continuous flow of pure krypton, at a rate of 0.82 $\text{cm}^3 \text{min}^{-1}$, and a pressure of $3.3 \times 10^3 \text{ Pa}$. In these conditions, the plasma emission lasted for 150 μs . The gas was pre-ionized in order to obtain the best discharge reliability. Spectroscopic and interferometric end-on measurements have been made simultaneously through the plasma life, and have been taken 2 mm off the lamp axis, and from symmetrical positions referred to it. The high axial homogeneity and the very good cylindrical symmetry of electron density and temperature in this lamp [12] allow this.

The lamp is placed in one of the arms of a Twyman-Green interferometer simultaneously illuminated with two He-Ne lasers (543.0 nm and 632.8 nm) in order to determine the electron density evolution curve from the refractivity changes due to free electrons. The spectroscopic beam (defined by 2 mm pinholes separated by 1.5 m) is directed and focused onto the entrance slit of a Jobin-Yvon spectrometer 1.5 m focal length, 1200 lines mm^{-1} holographic grating), equipped with an optical multichannel analyser (OMA). This OMA has a detector array which is divided into 512 channels (EG&G 1455R-512-HQ). The dispersion was 12.59 pm/channel at 589.0 nm in the first order of diffraction. The spectrometer was very carefully calibrated in wavelength as well as in intensity with uncertainties lower than 1% and 4%, respectively [13,14]. Time exposures for the spectra were 5 μs .

Mirror M3 placed behind the plasma column was used to measure the optical depth and to detect possible self-absorption effects on each line profile. This is detected in any spectral line if the intensities ratio between the spectrum taken with the mirror and without it is lower at the peak than at any other part of the profile [14]. Self absorption was detected in less than 20% of the whole spectral profiles, and in less than 10% of these cases the reconstructed profile differed from the measured one without the mirror by more than 20% in the peak intensity. These profiles have been rejected from further calculations.

The experiment consists of end-on measurements of some of the Kr II lines emitted by the plasma in the visible region (390–720 nm). Each spectral interval (see Fig. 2) has been recorded at 12 different instants within the first 130 μs of the plasma lifetime. All lines were registered in the first order of diffraction of the spectrometer, the most efficient.

III. PLASMA DIAGNOSTICS

Figure 3 shows the electron density evolution determined from two-wavelength interferometry (543.0 and 632.8 nm) corresponding to the He-Ne lasers. Up to 60 interferograms

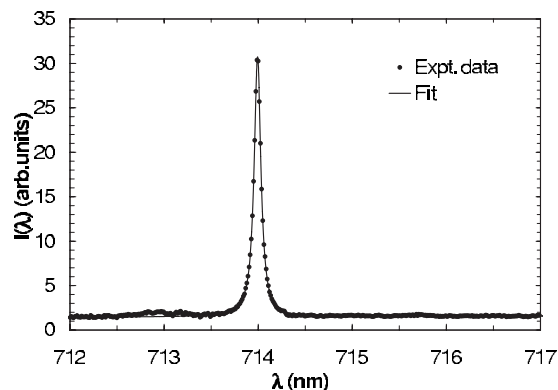


FIG. 2. An example of the experimental spectrum of Kr II 713.999 nm line and its corresponding fit at the instant 50 μs of the plasma life.

for both wavelengths were taken in the middle of the experiment, all of them 500 μs long. For each interferogram the phase evolution has been extracted [15]. Hence, the electron density curve $N_e(t)$ was obtained [11] assuming that the plasma column length was equal to the lamp length. The electron density uncertainty estimated by this technique is lower than 10%.

In collision-dominated plasmas, as is the case of this experiment, it is a common hypothesis to assume that excitation temperature and kinetic electron temperature take similar values [16]. In this work, we have determined the Kr II excitation temperature (see Fig. 4) from the slope of a Boltzmann plot calculated for each instant of the plasma life with the intensities of 8 selected Kr II lines whose transition probabilities are previously known [6].

In relation to spectroscopic data processing, all the spectra were divided by the spectrometer transmittance function and fitted to sums of Lorentzian functions plus a luminous background with a linear dependence [11]. Differences between the experimental spectra and the fits were usually lower than 1% (Fig. 2). These fitting algorithms allow us to determine simultaneously the center, asymmetry, line width [full width

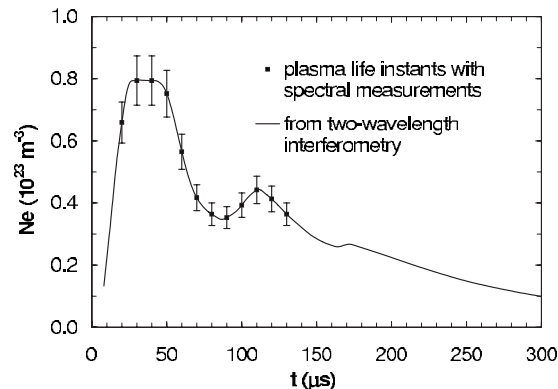


FIG. 3. Electron density evolution measured from two-wavelength interferometry. Error bars of 10% have been depicted in every point corresponding to the plasma lifetime instants where the Kr II spectral lines have been registered.

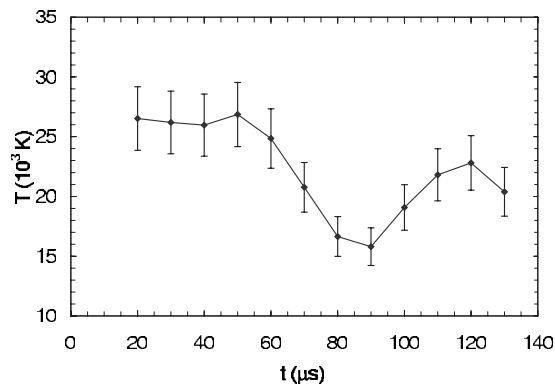


FIG. 4. Kr II excitation temperature obtained from Boltzmann plots. An uncertainty of 10% is estimated for temperature values.

at half maximum (FWHM)] and area of each profile.

In order to obtain the Stark width from the whole line width, other broadening mechanisms have also been taken into account. The instrumental width ω_i has been determined by measuring the FWHM of the entrance slit image when introducing a laser beam in the spectrometer. The measured value was three channels. The Doppler width ω_D was determined from the temperature obtained in the Boltzmann plots. Other broadening mechanisms as ionic, van der Waals, and resonance are negligibly small for our physical conditions [11]. After calculating the total Gaussian width component $\omega_G = (\omega_i^2 + \omega_D^2)^{1/2}$, a deconvolution procedure [17] allowed us to obtain the Stark widths ω_S from the experimental widths.

IV. RESULTS

As a first step, the different ω_S values measured at different instants of the plasma life for each line have been divided by the corresponding N_e value at that instant and have all been plotted vs the measured temperature T , in order to check possible dependencies of the Stark widths on this parameter. All the lines show the same behavior. In Fig. 5 the data measured in this work for the Kr II line 405.704 nm are shown. As can be seen from this figure no trends are ob-

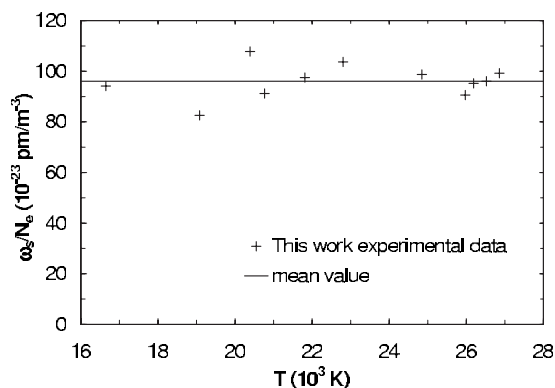


FIG. 5. Stark width to electron density ratio for the Kr II 405.704 nm spectral line vs temperature. No trends are observed in the temperature range of this experiment.

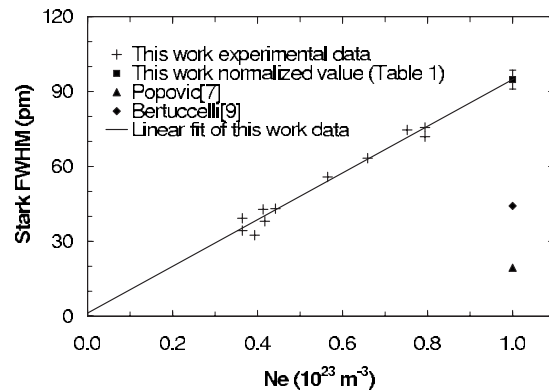


FIG. 6. Stark FWHM vs electron density N_e for the Kr II 405.704 nm spectral line. The normalized value at $N_e = 10^{23} \text{ m}^{-3}$ (those indicated in Table I) is included with its corresponding 4% statistical error bar obtained from the linear fit. Serious discrepancies can be observed between scarce literature values.

served, at least in the temperature range of this experiment and within the 10% uncertainty that can be assigned to measured data.

Since our ω_S/N_e ratios do not show clear dependencies with T , linear fits of Stark widths ω_S vs electron density N_e can be proposed as calibration functions for determining electron density in krypton plasmas. In Fig. 6, a linear fit for the Kr II line 405.704 nm is shown. Very good linear dependencies between the Stark width and the electron density have been observed for all the lines measured in this experiment. Hence, as the final results, we give in Table I the normalized Stark width values ω_m at electron density $N_e = 10^{23} \text{ m}^{-3}$ obtained as the expected value from the corresponding linear fit $\omega_m = A + BN_e$ for every spectral line. A mean temperature value of 21 000 K can be considered for this work Stark parameter values. Figure 6 also includes the other two available literature values for the Kr II line 405.704 nm, which have been normalized at electron density $N_e = 10^{23} \text{ m}^{-3}$. Clear discrepancies appear between these values.

In the case of Stark shifts d_S , they have been obtained for each line from the following procedure. A linear fit of the center wavelengths as a function of electron density is performed. Since the line center at vanishing electron density is not known, this is assumed to be the ordinate of such a plot at $N_e = 0$. By subtracting this value from all line centers and by multiplying afterwards this difference by the linear dispersion of the spectrometer, all d_S values are obtained for each line. Once more, the existence of very good linear dependencies between d_S and N_e has been proved. The linear fit of the Kr II line 405.704 nm is shown in Fig. 7.

In Table I, all Stark width and shift data obtained in this work are listed with others taken from the literature, all of them normalized at electron density $N_e = 10^{23} \text{ m}^{-3}$. In the first three columns, the information of the transition is given while in the fourth column the wavelengths are listed, always according to Striganov *et al.* [18] with the exception of the 447.501 nm line, for which the upper and lower energy levels seem to correspond to the $5s'-5p'$ transition [8,19]. The fifth and seventh columns contain, respectively, the Stark

TABLE I. Stark widths and shifts of the Kr II spectral lines measured in this work and the available literature values.

Transition array	Multiplet	J	λ (nm)	w_m (pm)	w_m (10^{11} s^{-1})	d_m (pm)	d_m (10^{11} s^{-1})	Reference			
4d-5p	$^4\text{D}-^2\text{D}^0$	5/2-5/2	507.723	57.2 (4)	4.18	-11.9 (8)	-0.87	This work			
	$^2\text{D}-^4\text{D}^0$	1/2-3/2	602.239	80.0 (5)	4.16			This work			
	$^4\text{D}-^4\text{D}^0$	7/2-5/2	630.366	97.1 (3)	4.61			This work			
		3/2-5/2	663.437	87.8 (5)	3.76			This work			
4d-5p'	$^4\text{D}-^4\text{P}^0$	1/2-1/2	713.999	99.7 (6)	3.69			This work			
	$^2\text{D}-^2\text{D}^0$	3/2-5/2	516.680	63.0 (4)	4.45			This work			
		3/2-3/2	520.022	142.0 (4)	9.90	-25.9 (3)	-1.81	This work			
	$^2\text{D}-^2\text{P}^0$	3/2-1/2	518.699	150.7 (3)	10.6	-34.2 (4)	-2.40	This work			
5s-5p	$^2\text{D}-^2\text{F}^0$	3/2-5/2	616.880	73.8 (5)	3.66	-5.7 (6)	-0.28	This work			
		5/2-7/2	660.501	78.5 (5)	3.39			This work			
	$^2\text{P}-^2\text{F}^0$	3/2-5/2	687.085	99.9 (4)	3.99			This work			
	$^4\text{P}-^4\text{P}^0$	1/2-3/2	599.222	54.2 (4)	2.85	-7.3 (2)	-0.38	This work			
5s'-5p'				44.6	2.34	-15.8	-0.83	[7]			
				51.8 (10)	2.72	-7.6 (13)	-0.40	[1]			
				94.8 (4)	10.9	-26.6 (6)	-3.05	This work			
				19.4	2.22	-52	-5.96	[7]			
				44.2 (C+)	5.06			[9]			
				109.5 (3)	10.6	-27.1 (4)	-2.61	This work			
				27	2.60	-6.72	-0.65	[7]			
				117.9 (4)	11.1	-25.9 (2)	-2.44	This work			
				27.9	2.63	-7.05	-0.66	[7]			
				31.0 (C+)	2.92	-1.03 (C+)	-0.10	[8]			
				$^2\text{D}-^2\text{D}^0$	3/2-3/2	406.513	81.5 (6)	9.30	-19.3 (3)	-2.20	This work
						19.3	2.20	-4.48	-0.51	[7]	
			44.2 (C+)	5.04			[9]				
			92.2 (5)	10.3	-17.1 (5)	-1.91	This work				
			19.9	2.22	-4.73	-0.53	[7]				
			39.2 (C+)	4.38			[9]				
			$^2\text{D}-^2\text{F}^0$	5/2-5/2	469.130	46.4 (6)	3.97		This work		
					35.9 (50)	3.07			[7]		
5s'-5p	$^2\text{D}-^2\text{S}^0$	3/2-1/2	677.120	85.7 (5)	3.52			This work			
	$^2\text{D}-^2\text{D}^0$	5/2-3/2	707.397	97.5 (4)	3.67			This work			
5p'-4d''	$^2\text{F}^0-^2\text{D}$	7/2-5/2	448.988	126.3 (4)	11.8	43.1 (5)	4.03	This work			
	$^2\text{P}^0-^2\text{D}$	3/2-5/2	459.280	158.5 (5)	14.2	75.7 (2)	6.76	This work			
	$^2\text{D}^0-^2\text{D}$	3/2-3/2	503.385	233.8 (3)	17.4	68.3 (2)	5.08	This work			
		5/2-5/2	508.652	145.9 (4)	10.6	64.6 (2)	4.71	This work			
5p-6s	$^4\text{P}^0-^4\text{P}$	3/2-3/2	423.664	104.4 (5)	11.0	39.0 (6)	4.10	This work			
		3/2-5/2	438.654	117.8 (5)	11.5	44.0 (4)	4.31	This work			
		1/2-3/2	452.314	133.6 (5)	12.3	52.9 (2)	4.87	This work			
	$^2\text{D}^0-^2\text{P}$	5/2-3/2	455.661	132.7 (4)	12.0	49.2 (5)	4.47	This work			
	$^4\text{D}^0-^4\text{P}$	5/2-3/2	458.284	124.4 (4)	11.1	50.6 (3)	4.54	This work			
	$^4\text{S}^0-^4\text{P}$	3/2-1/2	496.025	130.3 (4)	10.0	51.4 (3)	3.94	This work			
5p'-6s	$^2\text{S}^0-^2\text{P}$	1/2-1/2	494.850	202.8 (5)	15.6	64.6 (4)	4.97	This work			
4d'-5f'	$^2\text{D}-^2\text{F}^0$	5/2-5/2	527.650	209.5 (4)	14.2			This work			
5s''-5p''	$^2\text{S}-^2\text{P}^0$	1/2-1/2	445.321	68.0 (9)	6.46	-14.6 (7)	-1.39	This work			
5p-5d	$^2\text{S}^0-^4\text{D}$	1/2-3/2	514.305	110.0 (6)	7.84	30.0 (3)	2.14	This work			
5p'-5d	$^2\text{D}^0-^2\text{F}$	5/2-7/2	390.625	161.3 (5)	19.9			This work			
				41.9 (C+)	5.18			[9]			

width and shift data expressed in picometres obtained in this work, and data from other authors. The data uncertainties appeared between brackets and are expressed in percentages

for the data of this work, and with the qualifying letter (C⁺ = uncertainties within 40%) given by Konjevic *et al.* [5] in their last paper for the case of other author measurements.

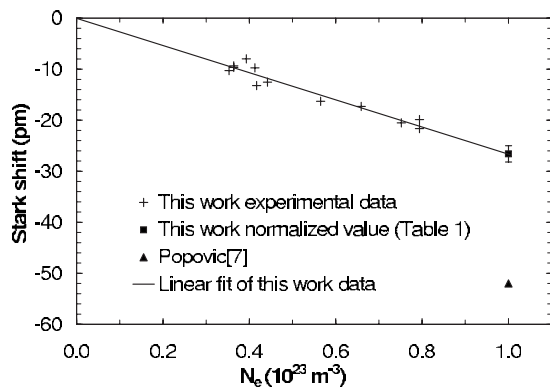


FIG. 7. Stark shift vs electron density Ne for the Kr II 405.704 nm spectral line. The normalized value at $N_e=10^{23} \text{ m}^{-3}$ (those indicated in Table I) is included with its corresponding 6% statistical error bar obtained from the linear fit.

The sixth and eighth columns contain the Stark parameters in frequency units in order to better compare the regularities within the same transition array. In the case of shifts, the expression employed to convert them from picometers to frequency units was $d(\text{s}^{-1})=2\pi(\text{ms}^{-1})[\lambda(\text{nm})]^{-2}d(\text{pm})10^6$, that is to say, in frequency units the positive sign has been preserved for red shifts and the negative one for blue shifts. Finally, the corresponding references are given in the last column.

An important remark should be made. The uncertainties of the date of this work are given from the statistical error obtained in the linear fits, all below 10%, which gives an idea of the very good linear dependencies of Stark parameters with electron density. Although taking into account a 10% uncertainty for the electron density measurements, an overall 10% to 15% uncertainty range, depending on the line, could be more realistic.

V. DISCUSSION

When comparing the Stark widths in frequency units of the spectral lines whose multiplets correspond to the first transition array ($4d-5p$) that is shown in Table I, a reasonable regularity appears (differences $<15\%$ from an average value of $4.1 \times 10^{11} \text{ s}^{-1}$).

When comparing the data of the six spectral lines corresponding to the second transition array ($4d-5p'$) of the Table I, the regularity is clearly broken by lines 518.699 nm and 520.022 nm. In Fig. 8 a scheme with some of the Kr II energy levels $5p'$ and their closest perturbing levels $4d'$ is shown by using the LS coupling scheme designations [19]. It is important to note that the LS coupling scheme is a good approximation for the levels with lower l in a singly ionized multielectronic atom. The upper transition levels of these two lines are, respectively, $5p'^2P^0_{1/2}$ and $5p'^2D^0_{3/2}$. Figure 8 shows that in both cases the perturbing effect of the near level $4d'^2P_{1/2}$ could explain the additional Stark broadening of these spectral lines (around $10.3 \times 10^{11} \text{ s}^{-1}$). Besides, for these two lines there is a great blue shift, (around $2.2 \times 10^{11} \text{ s}^{-1}$), which can be explained when considering that

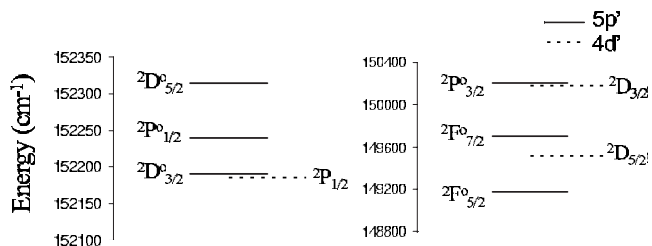


FIG. 8. Energy scheme of some $5p'$ Kr II levels in continuous line, and nearest perturbing levels $4d'$ in dashed line.

the perturbing level $4d'^2P_{1/2}$ is under upper level of the transitions. For the other four spectral lines of the transition array, whose $5p'^2D^0_{5/2}$, $2F^0_{5/2}$, and $2F^0_{7/2}$ upper levels are far from the perturbing $4d'$ levels, there is a reasonable regularity (differences $<15\%$ from an average value of $3.9 \times 10^{11} \text{ s}^{-1}$).

In the following transition array ($5s-5p$) with one measured spectral line, 599.222 nm, we can compare the new measurements with our previous work [1], finding very good agreement, taking into account the experimental uncertainties (discrepancies of 4% in Stark parameters). For that line there is also reasonable agreement (within 20%) with the Popovic *et al.* [7] theoretical value ($w_m/w_{th}=1.2$).

Popovic *et al.* theoretical data [7] have been taken for $N_e=10^{23} \text{ m}^{-3}$ and $T=20000 \text{ K}$ in order to better compare with the results of this work. These authors have used the modified semiempirical method [20], whose accuracy is assumed within $\pm 50\%$, to calculate Stark widths of 37 spectral lines from the $5s-5p$ and $5s'-5p'$ transition arrays of Kr II. In comparison with the semiclassical perturbation approach [21], the modified semiempirical method needs a considerably smaller number of atomic data. The accuracy of this method is linked to the absence of perturbing levels strongly violating the assumed approximations [20].

Just so, the greatest discrepancies between our measurements and the modified semiempirical method calculations appeared in the transition array $5s'-5p'$. As can be shown in Fig. 8, and taking into account the above discussion about the perturbing effect of $4d'$ levels, it is perfectly reasonable that the five spectral lines whose upper levels $5p'^2P^0_{1/2}$, $2D^0_{3/2}$, and $2P^0_{3/2}$ are perturbed, show the greatest Stark widths (around $10.4 \times 10^{11} \text{ s}^{-1}$) and also great blue shifts (around $2.4 \times 10^{11} \text{ s}^{-1}$). In all these cases our measurements are about a factor 4 above the modified semiempirical method calculations of Popovic *et al.* [7], because they do not take into account these perturbing levels. For the spectral line 469.130 nm, the only line in this transition whose upper level $5p'^2P^0_{5/2}$ is far from perturbing levels and for which a semiempirical calculation exists, the agreement with this calculation is reasonably good ($w_m/w_{th}=1.3$), giving the modified semiempirical method a value somewhat underestimated, as happened with 599.22 nm.

Only for the 447.501 nm spectral line, included between the perturbed transitions of the $5s'-5p'$ transition array, can we compare our measurements with those of Milosavljevic *et al.* [8]. These authors have measured several Kr II lines in a low-pressure pulsed arc end on in pure krypton. Line pro-

files were recorded on a shot-to-shot basis. The optical depth was checked by measuring the relative intensities of Kr II lines within the $5s^4P$ - $5p^4P^0$ multiplet and by comparing them with well-known intensity data. Agreement was obtained within the estimated uncertainties, thus indicating little or no self-absorption. The line profiles were corrected for instrumental and Doppler broadening. Their measurements correspond to an electron density of $1.65 \times 10^{23} \text{ m}^{-3}$ and a temperature of 17000 K. Their data are in satisfactory agreement with those calculated by Popovic *et al.* [7] with the modified semiempirical approach as can be seen in Table I for the line 447.501 nm. Their values for this Kr II line Stark width and shift are about a factor 4 and 3.5 below our values, respectively. We ignore the cause of this strong discrepancy.

For the transition array $5s'-5p'$, there is also three spectral lines corresponding to the group of perturbed upper levels, where we can compare our measurements with other available performed by Bertuccelli *et al.* [9]. These authors have measured a fairly large number of Kr II line widths using a low-pressure pulsed capillary discharge and a shot-to-shot technique, observing end on. Competing broadening mechanisms were found to be negligible, but instrumental broadening was taken into account. Their measurements correspond to an electron density of $0.265 \times 10^{23} \text{ m}^{-3}$ and a temperature of 14500 K, just below the ranges of our experiment. Although taking into account the different temperature ranges, their values are about a factor 2 below our width values. The difference is even greater for the $5p'-5d$ transition corresponding to the wavelength 390.625 nm, which appears at the end of the Table I. These differences can not be explained even with the uncertainty within 40% assigned to their work by Konjevic *et al.* [5], and also we ignore the cause of these discrepancies.

Within the following transition array ($5p'-4d''$) we can distinguish the two transitions whose lower levels $5p'^2P^0_{3/2}$ and $^2D^0_{3/2}$ are perturbed according to Fig. 8 as we have already discussed, and the two transitions whose lower levels $5p'^2F^0_{7/2}$ and $^2D^0_{5/2}$ are not perturbed. In the first case, the width and shift values are higher than the second case values, as can be expected. Moreover, as the perturbed levels are the lower levels of the transitions (the upper ones are not perturbed), in this case the upper and lower levels of the transi-

tion approach each other, hence there is an additional red shift in good agreement with the measurements performed. It is interesting to remark that the perturbing effect on the upper level is usually considered as the most relevant one. However, in this particular case the energy differences between the lower level of the transition and the perturbing level are just only 23.6 cm^{-1} for $^2P^0_{3/2}$ and 5.1 cm^{-1} for $^2D^0_{3/2}$. This is the reason why this perturbing effect has been possible to detect.

The following transition array ($5p$ - $6s$) shows a very good regularity for the six spectral lines which have been measured because they do not have neighboring perturbing levels. The width differences are lower than 13% from a mean value of $11.3 \times 10^{11} \text{ s}^{-1}$, while the shift differences are lower than 11% from a average value of $4.4 \times 10^{11} \text{ s}^{-1}$.

Finally, each one of the last five spectral lines of the Table I belong to different transitions arrays, so we can not analyze the Stark regularities.

VI. CONCLUSION

We have measured 35 Stark widths and 24 Stark shifts for a set of transitions of singly charged krypton. The greatest departures from regularity of some lines within the same multiplet or transition and also the greatest differences with the semiempirical calculations [7] can be explained taking into account the perturbing effect of some $4d'$ over $5p'$ levels due to the structure of the Kr II energy levels scheme. In other cases, there is a disagreement with the very scarce experimental data available from literature [8,9]. Hence, in conclusion we note the importance of supplying more measurements in order to get an accurate and reliable collection of these atomic parameters.

ACKNOWLEDGMENTS

We thank S González for his work in the experimental arrangement, and the Ministerio de Ciencia y Tecnología of Spain and the Consejería de Educación y Cultura de la Junta de Castilla y León for its financial support under contracts No. FIS2005-03155 and VA015A05 respectively. J. A. Aparicio is grateful to the Organización Nacional de Ciegos de España (ONCE) for their help.

-
- [1] A. de Castro, J. A. Aparicio, J. A. del Val, V. R. González, and S. Mar, *J. Phys. B* **34**, 3275 (2001).
 - [2] J. A. Cardelli and D. Meyer, *Astrophys. J.* **477**, L57 (1997).
 - [3] S. I. B. Cartledge, D. M. Meyer, and J. T. Lauroesch, *Astrophys. J.* **597**, 408 (2003).
 - [4] H. L. Dinerstein, *Astrophys. J.* **550**, L223 (2001).
 - [5] N. Konjevic, A. Lesage, J. R. Fuhr, and W. L. Wiese, *J. Phys. Chem. Ref. Data* **31**(3), 875 (2002).
 - [6] S. Mar, J. A. del Val, F. Rodríguez, R. J. Peláez, V. R. González, A. B. Gonzalo, A. de Castro, and J. A. Aparicio, *J. Phys. B* **39**, 3709 (2006).
 - [7] L. C. Popovic and M. S. Dimitrijevic, *Serb. Astron. J.* **161**, 89 (2000).
 - [8] V. M. Milosavjevic, S. Djenize, M. S. Dimitrijevic, and L. C. Popovic, *Phys. Rev. E* **62**, 4137 (2000).
 - [9] G. Bertuccelli and H. O. Di Rocco, *Phys. Scr.* **44**, 138 (1991).
 - [10] M. A. Gigosos, S. Mar, C. Pérez, and I. de la Rosa, *Phys. Rev. E* **49**, 1575 (1994).
 - [11] S. Djurovic, R. J. Peláez, M. Cirisan, J. A. Aparicio, and S. Mar, *J. Phys. B* **39**, 2901 (2006).
 - [12] J. A. del Val, S. Mar, M. A. Gigosos, I. de la Rosa, C. Pérez, and V. R. González, *Jpn. J. Appl. Phys., Part 1* **37**, 4177 (1998).
 - [13] V. R. González, Ph.D. thesis, Universidad de Valladolid, 1999 (unpublished).
 - [14] V. R. González, J. A. Aparicio, J. A. del Val, and S. Mar,

- Astron. Astrophys. **363**, 1177 (2000).
- [15] M. I. de la Rosa Garcia, M. C. Pérez Garcia, A. M. de Frutos Baraja, and S. Mar Sardana, Phys. Rev. A **42**, 7389 (1990).
- [16] J. A. M. Van der Mullen, Phys. Rep. **191**, 109 (1990).
- [17] J. T. Davies and J. M. Vaughan, Astrophys. J. **4**, 1302 (1963).
- [18] A. R. Striganov and N. S. Sventitskii, *Tables of Spectral Lines of Neutral and Ionised Atoms* (Plenum, New York, 1968).
- [19] J. Sugar and A. J. Musgrove, J. Phys. Chem. Ref. Data **20**, 859 (1991).
- [20] M. S. Dimitrijevic and N. Konjevic, J. Quant. Spectrosc. Radiat. Transf. **24**, 451 (1980).
- [21] H. R. Griem, *Spectral Line Broadening by Plasmas* (Academic, New York, 1974).